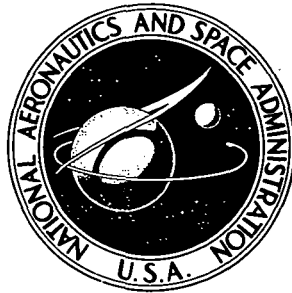


NASA TECHNICAL NOTE



N73-18541

NASA TN D-7209

NASA TN D-7209

CASE FILE  
COPY

MICROSTRUCTURAL STUDY OF  
THE NICKEL-BASE ALLOY WAZ-20  
USING QUALITATIVE AND QUANTITATIVE  
ELECTRON OPTICAL TECHNIQUES

*by Stanley G. Young*

*Lewis Research Center*

*Cleveland, Ohio 44135*

1. Report No. <b>NASA TN D-7209</b>		2. Government Accession No.		3. Recipient's Catalog No.	
4. Title and Subtitle <b>MICROSTRUCTURAL STUDY OF THE NICKEL-BASE ALLOY WAZ-20 USING QUALITATIVE AND QUANTITATIVE ELECTRON OPTICAL TECHNIQUES</b>				5. Report Date <b>March 1973</b>	
				6. Performing Organization Code	
7. Author(s) <b>Stanley G. Young</b>				8. Performing Organization Report No. <b>E-7250</b>	
9. Performing Organization Name and Address <b>Lewis Research Center National Aeronautics and Space Administration Cleveland, Ohio 44135</b>				10. Work Unit No. <b>501-01</b>	
				11. Contract or Grant No.	
12. Sponsoring Agency Name and Address <b>National Aeronautics and Space Administration Washington, D. C. 20546</b>				13. Type of Report and Period Covered <b>Technical Note</b>	
				14. Sponsoring Agency Code	
15. Supplementary Notes					
16. Abstract <p>The NASA nickel-base alloy WAZ-20 was analyzed by advanced metallographic techniques to qualitatively and quantitatively characterize its phases and stability. The as-cast alloy contained primary gamma-prime, a coarse gamma-gamma prime eutectic, a gamma-fine gamma prime matrix, and MC carbides. A specimen aged at 870<sup>0</sup> C for 1000 hours contained these same constituents and a few widely scattered high W particles. No detrimental phases (such as sigma or mu) were observed. Scanning electron microscope, light metallography, and replica electron microscope methods are compared. The value of quantitative electron microprobe techniques such as spot and area analysis is demonstrated.</p>					
17. Key Words (Suggested by Author(s)) <b>Microstructure; Alloy phases; Nickel-base alloys; WAZ-20; Analytical techniques; Characterization; Scanning electron microscope; Electron microprobe; X-ray diffraction analysis; Metallography; Stability</b>			18. Distribution Statement <b>Unclassified - unlimited</b>		
19. Security Classif. (of this report) <b>Unclassified</b>		20. Security Classif. (of this page) <b>Unclassified</b>		21. No. of Pages <b>28</b>	22. Price* <b>\$3.00</b>

\* For sale by the National Technical Information Service, Springfield, Virginia 22151

MICROSTRUCTURAL STUDY OF THE NICKEL-BASE ALLOY  
WAZ-20 USING QUALITATIVE AND QUANTITATIVE  
ELECTRON OPTICAL TECHNIQUES

by Stanley G. Young

Lewis Research Center

SUMMARY

The constituents of the NASA nickel-base alloy, WAZ-20, were studied by light metallography, scanning electron microscopy (SEM), and electron microprobe analysis (EMXA). The alloy was analyzed both in the as-cast condition and after aging for 1000 hours at 870<sup>o</sup> C to determine its stability. The composition of the constituents of the alloy were analyzed quantitatively using computer methods to correct the raw EMXA output for background, absorption, fluorescence, etc.

The as-cast alloy contained primary gamma prime, a gamma-fine gamma prime matrix, a coarse gamma-gamma prime constituent believed to be a eutectic and metal carbides (MC). The aged specimen contained all the constituents found in the as-cast specimen. Also a few high W particles were observed that appeared to have a M<sub>6</sub>C carbide chemistry. All the constituents except the carbides showed approximately the same chemistry after aging as observed in the as-cast condition. No detrimental phases were observed that could be expected to weaken the alloy or indicate lack of stability at the time and temperature exposures of this study.

Two observations were made regarding metallographic techniques. First, SEM photomicrographs at X1700, when compared with light photomicrographs at the same magnification, showed adequate resolution, so that features were visible that would normally have to be observed by the use of more expensive replica electron microscope techniques at equivalent magnifications. Second, an EMXA analysis of a single phase (gamma prime) obtained with a broad area scan yielded an analysis nearly identical to a point analysis of that phase. This suggests that, if the composition and area or volume percent of one phase of a two-phase region is known, the composition of the other phase can be calculated from an EMXA broad area analysis, even though it may be too small for direct EMXA quantitative analysis.

## INTRODUCTION

The lack of adequate materials for advanced turbine engines has limited operating temperatures and engine efficiency. The high-temperature limits are being extended, however, with the development of improved nickel (Ni) and cobalt (Co) based superalloys, and by the use of new processing techniques. The NASA Ni-base alloy, WAZ-20, was developed to permit higher engine temperatures and has been cast with both random and directional grain orientations (ref. 1). Both forms of WAZ-20 showed substantially higher tensile strength at 1205° C than most other known cast Ni-base alloys. Certain strength properties, such as intermediate-temperature tensile strength, ductility, and stress-rupture life, of the directional polycrystalline form exceeded those of random WAZ-20. The 100-hour use temperatures at 103.4 meganewtons per square meter (15 000 psi) are 1063° C for the directional polycrystalline material, and 1038° C for the random polycrystalline material. In addition, WAZ-20 has excellent room-temperature Charpy impact strengths both as-cast and after aging.

The WAZ-20 alloy also was shown to possess limited workability potential. A 0.33-centimeter chill cast slab of the random crystalline form was hot rolled to a thickness of 0.05 centimeter in a conventional rolling mill.

WAZ-20 has a melting point higher than most presently known Ni-base systems because of its high tungsten (W) content and because it contains relatively few alloying constituents as contrasted to most other nickel base alloys. Other alloying constituents include aluminum (Al), carbon (C) and zirconium (Zr) in the most favorable combination consistent with maintaining a high melting point and achieving sound castings with relatively little segregation (ref. 1). The nominal chemistry range and chemical analyses are presented in table I.

Previous metallographic studies on this alloy were limited primarily to light microscopy metallographic evaluation of the structure. The object of this work was, therefore, to more completely characterize the constituent phases, by the application of electron microscopy and electron microprobe analysis techniques, and at the same time to demonstrate and expand the capabilities of the advanced metallographic techniques used. Electron optical techniques have recently been applied to the study of many Ni and Co alloys and alloy-coating systems (refs. 2 to 6). The directionally solidified form of the WAZ-20 alloy was used for this study in both the

as-cast condition and after aging for 1000 hours at 870<sup>o</sup> C to determine its micro-structural and chemical stability.

The alloy was examined by means of the scanning electron microscope (SEM); the resulting photomicrographs were compared with both light photomicrographs and replica electron photomicrographs. The electron microprobe X-ray analyzer (EMXA) was used to show the chemical composition of the phases present on a qualitative basis by exhibiting X-ray raster scans of the elements present and on a quantitative basis by analyzing each individual phase. Recently developed computer correction methods were applied to yield atom percent and weight percent compositions from the raw EMXA data. The structures of extracted carbide phases were identified by X-ray diffraction analysis. The results of the studies are presented with comparisons between the as-cast and aged materials.

## MATERIALS AND TECHNIQUES

### Materials

The chemical composition of WAZ-20 is given in table I (ref. 1). The nominal composition is included with chemical analyses made by an independent laboratory of typical heats of directionally solidified polycrystalline WAZ-20. Argon induction melted ingots were remelted and again cast into ingots under vacuum. They were then remelted under vacuum and cast in the directional solidification apparatus described in reference 7. The apparatus consisted of a three-zone resistance mold heater that surrounded a refractory shell mold. A copper chill block extended into the lower portion of the shell mold to establish grain growth directions. Rupture and tensile bars were cast with a gage length of 3.05 centimeters and a gage diameter of 6.35 millimeters. The tungsten and aluminum are near the low sides of the specified nominal values because of small losses during each of the three melting processes. Zirconium increased to the high side of the specified nominal values because this element and other trace elements were picked up from crucibles during induction melting. The same WAZ-20 material was used for studies of the effects of aging at 870<sup>o</sup> C (1600<sup>o</sup> F) for 1000 hours.

### Metallographic Preparation

Specimens used for the metallographic studies were cut perpendicular to the

growth direction. Previous work (ref. 1), showed that sections cut both parallel and perpendicular to the growth direction showed the same general features. Specimens were etched in a solution that was 92 parts hydrochloric acid, three parts, nitric acid, and five parts sulfuric acid. Photomicrographs were made by light microscopy, SEM (secondary and backscatter modes), and EMXA (backscatter and X-ray modes). The specimens were then repolished to prepare them for the quantitative EMXA studies. Specimens were often repolished to remove carbonaceous contamination that was deposited by the EMXA.

### Scanning Electron Microscopy

Scanning electron microscope (SEM) microphotographs in backscatter-electron and secondary-electron modes and light photomicrographs were made at the same magnifications of the same sample areas. Secondary electrons are emitted from near the surface and result in a photomicrograph revealing predominantly surface topography. The backscatter electrons are released from deeper within the specimen and result in a photomicrograph that is semiquantitative: the heavier elements emit more electrons than the lighter elements and thus phases containing the high atomic number elements appear lighter than the phases containing lower atomic number elements. Higher magnification SEM photomicrographs were compared with replica electron photomicrographs from the transmission electron microscope (TEM) to determine similarities. The three techniques for examining structures at high magnification differ in several ways; however, only their approximate resolution limitations are indicated here. For light microscopy, this may be considered to be 0.5 micrometer, for the SEM 0.03 micrometer, and for the replica TEM 0.005 micrometer.

### Electron Microprobe X-ray Analysis

The electron microprobe X-ray analyzer (EMXA) was used to provide backscatter photomicrographs and X-ray raster photomicrographs of each element in the specimens. The X-ray raster photomicrographs are rectangular (TV) raster patterns, in which counts of the desired X-rays were accumulated. This technique provides an average analysis over the area (raster) swept by the electron beam. In the EMXA spot analysis, the electron beam is narrowed as finely as possible,

usually to a spot approximately 1 to 2 micrometers in diameter. The EMXA was also used for quantitative determination of the composition of each phase or constituent observed in the specimens.

To obtain a quantitative analysis of the phases, a Colby microprobe analysis general intensity correction (MAGIC) computer program (ref. 8) was used to correct the raw EMXA data. The program was modified for use with a time sharing computer system, which allowed input from a remote typewriter terminal. Briefly, input to the program consisted of the chemical abbreviations of all elements in the specimen, characteristic X-ray lines analyzed, background and X-ray counts for high-purity standards of each element, and background and X-ray counts for each element in each microconstituent analyzed.

In this program the X-ray counts of each unknown in the specimen were compared with X-ray counts of high purity standards of each element (X-ray intensity ratio). Input data were corrected for background, counter dead time, absorption, fluorescence, backscatter, and ionization penetration. The MAGIC program often allowed overcorrection of the amount of absorption of X-rays from lighter elements such as carbon. As a result these lighter elements would be multiplied by a factor in the original MAGIC program that would increase them by unreasonably large amounts. Therefore, we established an empirical factor that would limit the amount of correction for absorption using analyses of known carbides and a well-characterized nickel aluminide (NiAl) reference material as standards. This factor never allowed the theoretical fraction of radiation emerging from the specimen to be reduced by more than 46 percent for any element during the iterative process of the computer program. Carbon was the only element influenced to any extent by this empirical factor.

The estimated error for our analyses using the modified MAGIC program varied inversely with the atomic number and amount of element present. For example, Ni was considered to be accurate within about 2 percent of the amount present, but the analyses of the lighter elements (C, Al, Si) are not considered to be more accurate than 10 percent of the amounts present. Detailed descriptions of electron beam microanalysis and correction procedures can be found in references 8 and 9.

### Electrolytic Extraction

The extraction procedure used for the carbides was essentially the same as that

suggested by the ASTM Committee E-4 and that used in references 10 and 11. The apparatus used for the extraction consisted of a direct-current power supply, which produced a current of approximately 200 milliamps between electrodes in a 10 percent solution of hydrochloric acid in methanol. A 1- by 1- by 0.25-centimeter specimen attached to a platinum wire was used as the anode, and a cylindrical platinum screen served as the cathode. The solution was contained in a 250-milliliter glass beaker. The total carbide phases that were separated were weighed and submitted for X-ray analysis. Procedures were essentially the same for both the as-cast and the aged materials.

## RESULTS AND DISCUSSION

### Microstructure of As-Cast Directionally Solidified WAZ-20

Metallography. - Light photomicrographs of the as-cast WAZ-20 specimens are shown in figure 1, at magnifications of X100, X250, and X500 and in figure 2(a) at X1700. These different magnifications were included to show relationships with electron optical photomicrographs at the same magnifications shown later in this section. In figure 1(a) at X100, microhardness indentations can be seen. These were used as locators for the specific areas to be examined by the electron optical methods. General features of the microstructure include: a gamma matrix containing a gamma prime precipitate and large primary gamma prime nodules with small angular carbides scattered throughout (ref. 1). The gamma-gamma prime structure is present in two forms: fine structured regions (gamma-fine gamma prime matrix), and coarser eutectic regions associated with or near the boundaries of the large primary gamma prime particles. Carbides also seem to be generally associated with the eutectic regions rather than occurring isolated within gamma-fine gamma prime matrix regions.

The X500 photomicrograph of figure 1(c) shows a single primary gamma prime nodule, the surrounding eutectic region, and several carbide particles. All of these are surrounded by the gamma-fine gamma prime matrix structure. This area of the sample, at this magnification, will be compared with backscatter-electron and X-ray raster photomicrographs taken with the EMXA (shown in the next section).

Figure 2 shows X1700 photomicrographs of part of the same area as shown in figure 1. Figure 2(a) was taken with an oil immersion objective lens at X1700 on a



light microscope, and figure 2(b) was taken on the SEM in the secondary-electron mode. Figure 2(b) shows that photomicrographs may be made with the SEM with much greater resolution than is possible with light optics because of the inherently higher resolution and the much greater depth of field of the SEM. The same metallographic mount was used, and there were no differences in surface preparation between these two photomicrographs.

The SEM photomicrograph was taken with the specimen at a  $20^{\circ}$  tilt, allowing highlighting of raised areas. The carbide particle in the upper left of the picture in figure 2(b) is raised above the surface. The gamma phase is also raised above the gamma prime phase because the gamma prime phase was more susceptible to attack by the etchant. The bright area in the lower part of the photomicrograph (fig. 2(b)) is a small pit that is clearly evident in the SEM photomicrograph but is unresolved in the corresponding light photomicrograph. The bright contrast is due to excessive electron scattering in this rough area, which contains thin discontinuous features. The increased resolution and depth of field in the SEM are responsible for the details revealed inside of the pit. Also note the clear resolution of the gamma-fine gamma prime region.

The secondary-electron mode on the SEM emphasizes surface topography. The SEM can also be operated in the backscatter electron (BSE) mode. In this mode the heavier elements emit more electrons than lighter elements and phases containing heavy elements show up lighter in the photomicrographs than those containing the lighter elements; thus (BSE) photomicrographs allow a semiquantitative first look at the specimen chemistry.

Figure 3 shows the same area as displayed in figure 2, taken in the BSE mode at a  $20^{\circ}$  tilt. Detail in the "holes" is not as clearly defined by this technique because of its strong oblique illumination effect; thus the pit shows up dark. The carbide shows up very light and must therefore contain a higher percentage of heavy elements than any other phase present. The gamma phase is lighter than the gamma prime. Although this could be partly a topographic effect (the specimen was etched), it is believed that the gamma contains a greater percentage of heavier elements than the gamma prime. A light band appeared across the gamma prime in the center of this photomicrograph. It may be a submerged phase, slightly below the sample surface, of higher average atomic number than the gamma prime (possibly gamma).

Figure 4 shows X5000 SEM photomicrographs of the same area of the specimen. Figure 4(a) shows a carbide, and 4(b) shows the interface between the coarse gamma-gamma prime eutectic and the fine structure. These photomicrographs can be compared with figure 5, which is a X6000 TEM photomicrograph of a replica from an area similar to that shown in figures 1 to 4. At this magnification very little additional information was obtained by the considerably more expensive method of replica electron microscopy than was obtained from the SEM photomicrograph. However, the value of the replica technique is apparent in figure 6, which shows a replica TEM photomicrograph at X17000 of the gamma-fine gamma prime matrix. An even finer precipitate (presumably also gamma prime) was observed in the gamma phase.

Electron microprobe X-ray analysis. - Qualitative and quantitative EMXA studies were made on the specimens. The qualitative studies consisted of spectral scans to identify the elements present and of BSE and X-ray raster photomicrographs of the areas previously studied by light microscopy to show the relative concentrations of the elements in the phases. Quantitative studies consisted of both spot analysis and raster area analysis of constituents of the specimen and correction of the intensity ratio results by means of the modified Colby computer program described previously.

Figure 7 shows a backscatter photomicrograph and five X-ray raster photomicrographs at X500 of the specimen area shown in the light photomicrograph of figure 1(c). X-ray raster photomicrographs for C, W, Zr, Ni, and Al are shown for this area in figure 7. (Any lighter area in the BSE photomicrograph indicates higher concentration of heavy elements.) In X-ray raster photomicrographs for a particular element, lighter areas indicate locally higher concentrations of that element. From the X-ray raster photomicrographs, carbides were noted to be high in W and Zr, and noticeably low in Ni and Al. Carbon differences did not show up clearly in the X-ray photomicrographs, but did show up in the more sensitive quantitative results reported later. Carbon is difficult to separate from the background because it has a very low, broad peak (X-ray intensity against wavelength), and also because carbonaceous contamination deposits form where the beam impinges on the specimen. These deposits can increase the carbon X-ray count rate and can mask microstructural differences.

The X-ray raster photomicrographs did not clearly indicate differences between

gamma and gamma prime in individual element concentration, but the BSE photomicrograph (fig. 7(a)) showed the primary gamma prime to be slightly lower in heavy elements than the gamma phase. This was further substantiated by the quantitative measurements. A light-to-dark change was seen through the gamma prime region of the X500 photomicrograph of figure 7(a) (indicated), which seemed to separate the primary gamma prime from the gamma prime associated with the eutectic. This was noted in about the same location of the possible submerged gamma phase (indicated by the band) mentioned earlier (see fig. 3 at X1700).

Quantitative studies were made to determine element concentrations in each phase or region of the alloy. The raw EMXA results were computer corrected for the various effects mentioned previously.

Figure 8 shows light photomicrographs of the as-cast specimen. The areas examined by the microprobe are indicated in the etched specimen (fig. 8(a)). Carbonaceous contamination deposits delineating the regions scanned in EMXA study can be seen on the unetched polished specimen in figure 8(b).

Table II shows the analysis of the constituents of the as-cast WAZ-20 shown in figure 8. Table II(a) shows the analysis in terms of weight percent and table II(b) in terms of atomic percent. The final results shown in both tables were normalized to 100 percent in an attempt to make up for small errors in the original analysis and correction procedures. Also, percentages were rounded to the nearest 0.1 percent. In all cases for the as-cast WAZ-20, the total element content analyzed before normalizing was approximately 93 to 95 percent except for the carbide which resulted in about 85 percent total element content. Three general reasons may contribute to this incomplete accountability of all the elements present. First, a limiting factor (as previously noted) was intentionally placed on the absorption correction in the computer program to prevent it from overcorrecting small amounts of light elements by unreasonably large numbers. Second, with the instrument used, only three elements could be analyzed at a time, and the operating conditions between groups of three can be slightly different because of instrumental drift or other potential variables in the raw X-ray count analysis by the EMXA. Finally, if long time analyses are made, carbonaceous contamination builds up on the surface during the analysis. This causes an overall reduction in X-ray count rates from the specimen (for all elements except carbon) that is very difficult to correct. The carbon percent will increase and the other element percents will decrease by this process. Examples

of the carbonaceous contamination can be seen in the polished, unetched specimen of figure 8(b).

From table II several observations can be made. The carbide was observed to be a very high Zr, high W, carbide. X-ray diffraction of the extracted carbides indicated that they were a MC type.

Analysis of the gamma prime was done on both a spot (2- to 3- $\mu$ m diam) and on an area basis (30- by 26- $\mu$ m area), with all the EMXA conditions held constant. In both cases the analysis was essentially the same. This suggests that a two-phase region could be area scanned by EMXA to obtain its average analysis. Then, if the composition of one phase and the volume percent of the phases present were known or estimated by other methods, the composition of the unknown phase could be calculated, even though it might be too small for direct EMXA quantitative analysis. The known phase must, of course, be free from major chemical gradients or changes throughout the area analyzed.

The gamma-fine gamma prime matrix was analyzed by area scanning and found to be lower in Al and Zr, about the same in Ni and Si, and higher in W than the gamma prime. Carbon was noticeably higher in the gamma prime than in the gamma plus gamma prime regions but this was believed to be due to carbonaceous contamination buildup during analysis or to carbides submerged beneath the gamma-prime area being scanned. The eutectic region had an overall chemistry between the primary gamma prime and the gamma-fine gamma prime matrix.

#### Microstructure of Aged Directionally Solidified WAZ-20

Metallography. - Light photomicrographs of the aged directionally solidified WAZ-20 specimens are shown in figure 9 at X100, X250, and X500. This specimen was aged for 1000 hours at 870<sup>0</sup> C. In figure 9(a) at X100, a microhardness indentation can be seen, which, as in the case of the as-cast specimen, was used as a locator for the specific area to be examined by electron optical methods. At X250 the general features were similar to those of the as-cast specimen. No embrittling phases such as sigma or mu were observed after aging. Coarsening of the primary gamma prime was evident, and the regions adjacent to the primary gamma prime in the gamma-fine gamma prime matrix appear to have become somewhat enriched in gamma prime. Less of the eutectic was observed after aging. A new type of angular particle was observed in addition to the MC carbides. One large example of this new

type of particle can be seen in the lower left of the photomicrograph (fig. 9(b)). The smaller MC carbides are scattered around the edges of the gamma prime phase.

Figure 9(c) at X500 shows the large angular particle imbedded in a primary gamma prime nodule. Smaller carbides can be seen at the edge of the primary gamma prime particle, and are often associated with voids or etching pits. The surrounding gamma-fine gamma prime matrix comprises the remaining area shown in this photomicrograph. This region at this magnification was used for later electron optical studies of each constituent indicated.

Electron microprobe X-ray analysis. - The aged specimen was analyzed in much the same manner as described previously for the as-cast specimen. Qualitative and quantitative studies were made on the specimen. Qualitative analysis consisted of spectral scans to identify elements present. Quantitative studies consisted of both spot and area analysis of regions within the specimen and computer correction of the X-ray intensity ratio results.

Table III shows the results of the quantitative analysis of the aged WAZ-20 based on computer-corrected and normalized EMXA data. Table III(a) shows the results in terms of weight percent, and table III(b) in terms of atomic percent. As in the case for the as-cast WAZ-20, the total element contents of each constituent in the aged specimen, except for the carbide, were greater than 92 percent before normalizing to 100 percent. The results for the carbide in this case are considered questionable because only 66 percent of the element content was accounted for. The spectral scans did not indicate any other elements present. Therefore, it must be assumed that the most likely cause for this discrepancy is the presence of voids associated with the small carbide particles. The EMXA analysis depends on depth much more than on area. If only a thin layer of carbide were present here, other phases and/or subsurface voids could interfere with the analysis. Many other possibilities could contribute to this error such as slight misalignment of the spectrometers, and changing EMXA operating conditions. However, as previously mentioned, all other constituents of the as-cast and aged specimens were in good agreement with regard to the total element content.

From table III the following observations were made: The analysis for primary gamma prime and the gamma-fine gamma prime matrix were strikingly similar in the as-cast and aged specimens, except that the gamma-fine gamma prime matrix adjacent to the primary gamma prime has become slightly (less than 4 wt.%) enriched

in W. The eutectic was not analyzed in the aged specimen for two reasons : First, the eutectic regions were smaller , and an area scan analysis was not able to take in as representative an area as in the case of the as-cast specimen . Second , the similarity of both analyses of the primary gamma prime and the gamma-fine gamma prime matrix in the aged and as-cast specimens led to the further assumption that the eutectic would not change significantly (the eutectic had a chemistry generally between the above two mentioned constituents in the as-cast specimen) . The large angular particle , found in the aged specimen , contained nearly 75 percent W and approximately 22 percent Ni . This particle appeared to be a  $M_6C$  precipitate on a stoichiometric basis , but X-ray diffraction of the extracted carbides indicated only MC carbides , as in the case of the as-cast specimen . Perhaps there was too little of this type of carbide , or perhaps it is not a carbide but rather an intermetallic phase that was dissolved in the extraction process . In any case , no phases such as sigma or mu were observed that would be expected to weaken the alloy or indicate a detrimental lack of stability after the  $870^{\circ}C$  , 1000-hour exposure .

#### SUMMARY OF RESULTS

The constituent phases of the NASA Ni-base alloy , WAZ-20 , have been analyzed by light metallography , scanning electron microscopy , and electron microprobe X-ray analysis (EMXA) . The alloy was analyzed in both the as-cast condition and after aging for 1000 hours at  $870^{\circ}C$  . The following results were obtained:

1. The as-cast alloy consisted of primary gamma prime; a gamma-fine gamma prime matrix , which was higher in W , lower in Zr and aluminum (Al) , and about the same in nickel (Ni) and silicon (Si) as the primary gamma prime; coarse gamma-gamma prime eutectic with a chemistry generally between that of the primary gamma prime and the gamma-fine gamma prime matrix; and metal carbides (MC) , high in zirconium (Zr) and tungsten (W) .

2. The aged specimen also contained the same phases as the as-cast specimen . The gamma prime and the gamma-fine gamma prime matrix showed approximately the same chemistry after aging as observed in the as-cast condition . Less of the eutectic phase was observed after aging . In addition to the MC carbide particles , a few angular particles of very high W content were noted . These appeared to be a  $M_6C$  carbide , but , most likely because of their scarcity , they were not observed by X-ray diffraction in the extraction studies .

3. No detrimental phases such as sigma or mu, which would be expected to weaken the alloy or indicate lack of stability after extended high-temperature exposure, were observed with the time and exposure temperature of this study.

4. Scanning electron photomicrographs at X1700 were compared with light photomicrographs. The resolution by the SEM was adequate so that features were visible that would normally have to be observed by use of the more expensive replica electron microscope techniques at equivalent or somewhat higher magnifications.

5. An analysis of an area 30 by 26 micrometers obtained by raster scanning of a single phase (gamma prime) was found to yield a nearly identical analysis to a single point analysis of that phase (all other EMXA conditions held constant).

### CONCLUDING REMARKS

WAZ-20 can generally be classified as a gamma prime strengthened alloy with solid solution of W in the matrix for additional strengthening. The constituents of as-cast WAZ-20 were: primary gamma prime, a coarse gamma-gamma prime (believed to be a eutectic), a gamma-fine gamma prime matrix, and scattered MC carbides.

Although aging the alloy for 1000 hours at 870° C did not cause the precipitation of any phases such as sigma or mu that are generally detrimental to alloy strength, the analysis did indicate that aging may result in the formation of a small amount of  $M_6C$ . Further aging studies at other temperatures, under stress and for longer times, should be undertaken to completely verify its stability.

Part of the emphasis of this work was to expand and demonstrate the capabilities of the advanced metallographic techniques used. The results of scanning electron microscopy (SEM) were compared directly with light microscopy at X1700 and replica transmission electron microscopy (TEM) at higher magnifications. The resolution of the SEM photomicrographs was shown to be adequate so that features were visible that would normally have to be observed by the use of more expensive replica TEM techniques.

The results of the electron microprobe X-ray analyzer were computer corrected by a Colby MAGIC program with additional empirical corrections. Other MAGIC program versions have since been written by Colby. Several other programs have also been written by other investigators. Each will give slightly different quanti-

tative results, which are dependent on the various equations, assumptions, and constants used. No standard computer correction program exists as yet, and theory is currently being updated and improved in attempts to make the EMXA results more exact.

A method has been proposed herein that appears to make possible the quantitative analysis of phases too small to be analyzed by EMXA. An X-ray analysis using a broad area scan of a single phase (gamma prime) yielded a nearly identical analysis as a single point analysis of that phase (all other EMXA conditions held constant). The significance of this result is as follows: When a two-phase region is analyzed by EMXA using area (raster) electron beam scanning and when the composition and area or volume percent of one phase is known or estimated, the composition of the other phase can be calculated, even though it may be too small for direct EMXA quantitative analysis. Of course, the known phase must have nearly homogeneous composition, and the unknown region should be free from general concentration gradients. This method might also have application to analysis methods with wider beam spots, such as the ion beam mass spectrometer, or the ion scattering spectrometer.

Lewis Research Center,

National Aeronautics and Space Administration,

Cleveland, Ohio, December 8, 1972,

501-01.

#### REFERENCES

1. Waters, William J.; and Freche, John C.: A Nickel Base Alloy, WAZ-20, with Improved Strength in the 2000<sup>o</sup> to 2200<sup>o</sup> F Range. NASA TN D-5352, 1969.
2. Calhoun, C. D.: Development of Superalloys by Powder Metallurgy for use at 1000-1400 F. Rep. 71AEG248, General Electric Co. (NASA CR-72968), Nov. 1971.
3. Kent, William B.: Development Study of Compositions for Advanced Wrought Nickel-Base Superalloys. Rep. U-C-R-1055, Cyclops Corp. (NASA CR-120934), Jan. 1972.
4. Caves, Robert M.; and Grisaffe, Salvatore J.: Electron and Ion Microprobes Applied to Characterize and Aluminide Coating on IN-100. NASA TN D-6317, 1971.



5. Johnston, James R.; and Young, Stanley G.: Oxidation and Thermal Fatigue of Coated and Uncoated NX-188 Nickel-Base Alloy in a High-Velocity Gas Stream. NASA TN D-6795, 1972.
6. Radavich, John F.; and Coutts, Wilford H., Jr.: Metallography of the Super-Alloys. *Rev. High-Temp. Mat.*, vol. 1, no. 1, Aug. 1971, pp. 55-96.
7. Freche, John C.; Waters, William J.; and Ashbrook, Richard L.: Application of Directional Solidification to a NASA Nickel-Base Alloy (TAZ-8B). NASA TN D-4390, 1968.
8. Colby, J. W.: Quantitative Microprobe Analysis of Thin Insulating Films. *Advances in X-Ray Analysis*. Vol. 11. Plenum Press, 1968, pp. 287-303.
9. Beaman, D. R.; and Isasi, J. A.: Electron Beam Microanalysis. Part 1: The Fundamentals and Applications. *Mat. Res. Standards*, vol. 11, no. 11, Nov. 1971, p. 8; Part 2: Experimental Considerations and Qualitative Analysis. *Mat. Res. Standards*, vol. 11, no. 12, Dec. 1971. pp. 12-31, 51-56; also *Electron Beam Microanalysis*. Spec. Tech. Publ. No. 506, ASTM, 1972.
10. Kriege, Owen H.; and Sullivan, C. P.: The Separation of Gamma Prime from Udimet 700. *Trans. ASM*, vol. 61, no. 2, June 1968, pp. 278-282.
11. Kriege, Owen H.; and Baris, J. M.: The Chemical Partitioning of Elements in Gamma Prime Separated from Precipitation-Hardened, High-Temperature Nickel-Base Alloys. *Trans. ASM*, vol. 62, no. 1, Mar. 1969, pp. 195-200.

TABLE I. - ALLOY COMPOSITION<sup>a</sup>

Alloy	Composition, wt. %						
	W	Al	Zr	C	Ni	Si	B
WAZ-20 (nominal range)	17 - 20	6 - 7.0	1.4 - 1.6	0.10 - 0.20	Bal	-----	-----
Typical heats of directional polycrystalline WAZ-20 <sup>b</sup>	16.97	5.93	1.72	0.113	75.06	0.10	0.0003
	17.11	5.95	1.52	.113	75.08	.10	.0003
	17.90	5.85	1.70	.113	74.21	.11	.0003

<sup>a</sup>All data from ref. 1.

<sup>b</sup>Argon melted, followed by double vacuum remelt.

TABLE II. - ANALYSIS OF THE CONSTITUENTS OF AS CAST WAZ-20<sup>a</sup>

(a) Weight percent

(b) Atomic percent

Element	Composition, wt. %					Element	Composition, at. %				
	Carbide	Primary gamma prime		Gamma plus gamma prime			Carbide	Primary gamma prime		Gamma plus gamma prime	
		Spot	Area	Eutectic	Matrix			Spot	Area	Eutectic	Matrix
C	5.6	0.7 <sup>b</sup>	1.3 <sup>b</sup>	<.1	0.1	C	34.4	3.1 <sup>b</sup>	6.1 <sup>b</sup>	<.1	0.4
Al	.2	7.3	7.1	6.2	5.5	Al	.6	14.7	14.4	13.6	12.2
Si	<.1	.1	<.1	.1	<.1	Si	<.1	.2	.2	.2	.1
Ni	5.2	81.5	80.7	81.5	80.9	Ni	6.5	78.4	75.9	81.9	82.9
Zr	55.0	.8	.9	.9	.2	Zr	44.7	.5	.5	.6	.2
W	34.0	9.9	10.0	11.3	13.3	W	13.7	3.0	3.0	3.6	4.3

<sup>a</sup>Based on computer corrected and normalized EMXA data.

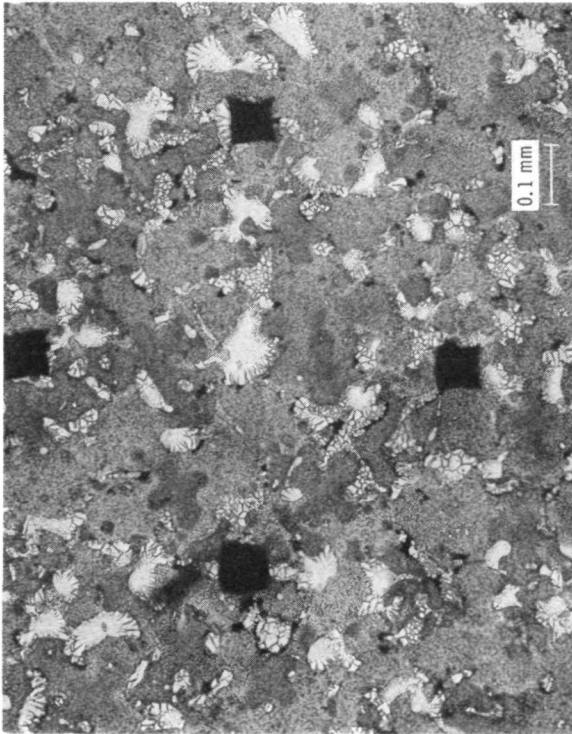
<sup>b</sup>This value may be high due to possible submerged carbides or carbon buildup during analysis.

TABLE III. - ANALYSIS OF THE CONSTITUENTS OF AGED WAZ -20<sup>a</sup>

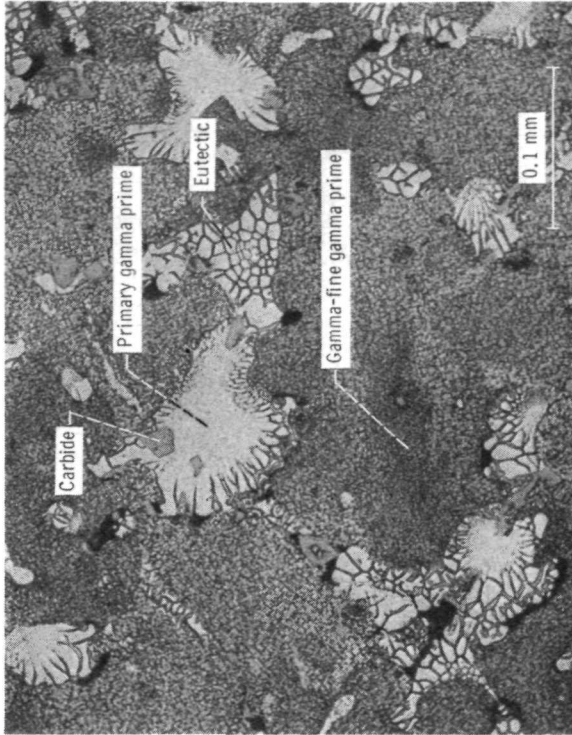
Element	(a) Weight percent				Element	(b) Atomic percent			
	Composition, wt. %					Composition, at. %			
	Carbide <sup>b</sup>	Primary gamma prime	Gamma plus gamma prime matrix	High W particle		Carbide <sup>b</sup>	Primary gamma prime	Gamma plus gamma prime matrix	High W particle
C	7.1	0.9	0.6	1.6	C	38.7	4.2	3.2	13.5
Al	.2	6.9	4.9	1.0	Al	.4	14.3	10.8	3.9
Si	.1	.1	<.1	.1	Si	.3	.3	.2	.4
Ni	5.6	81.6	79.1	22.4	Ni	6.3	77.8	80.7	39.5
Zr	65.3	1.0	.3	.6	Zr	46.7	.6	.2	.7
W	21.6	9.5	15.0	74.4	W	7.7	2.9	4.9	42.0

<sup>a</sup>Based on computer corrected and normalized EMXA data.

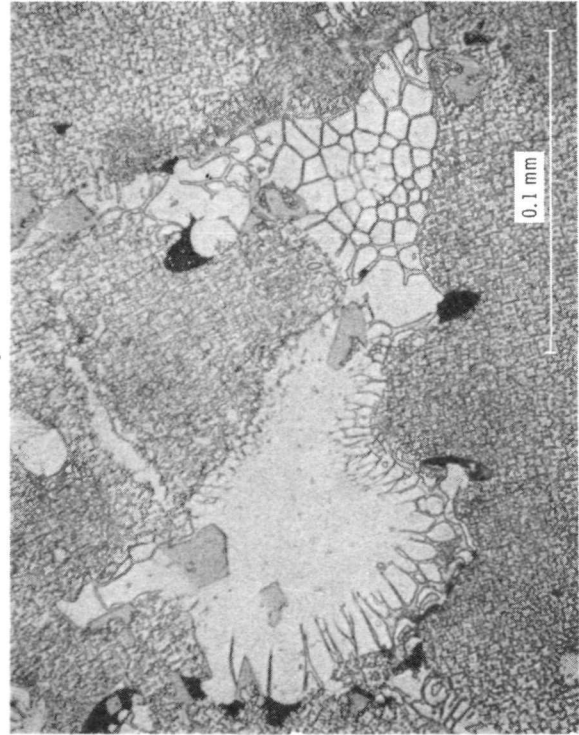
<sup>b</sup>The results for the carbide in this case are questionable, only 66 percent of the element content was accounted for. All other analyses totaled over 90 percent (raw wt. %).



(a) X100.

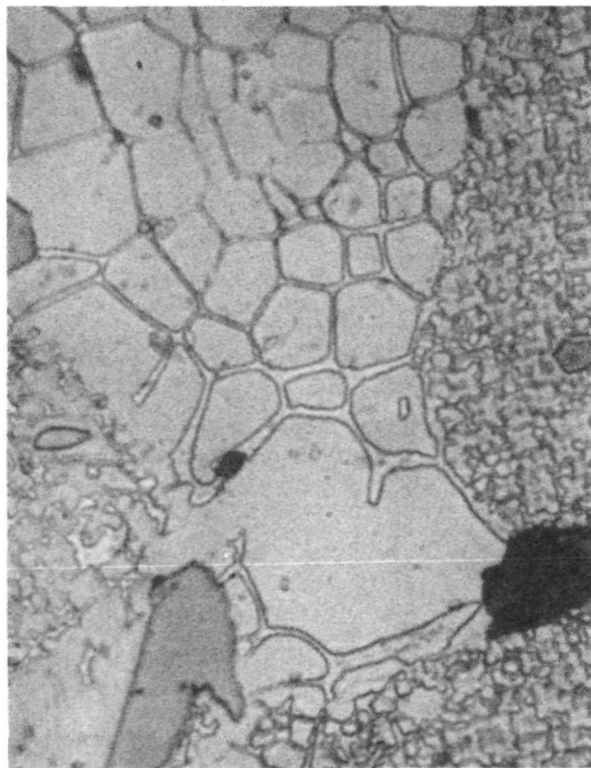


(b) X250.

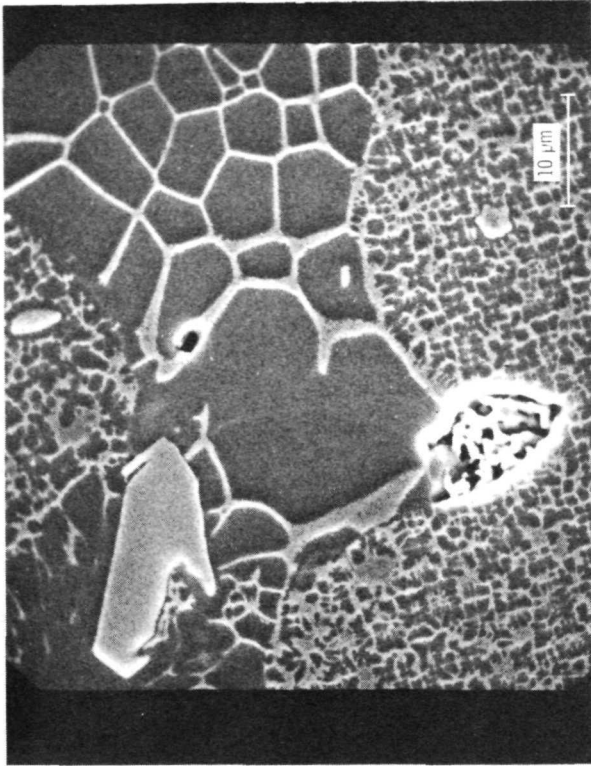


(c) X500.

Figure 1. - Light photomicrographs of as-cast, directionally solidified polycrystalline WAZ-20 at various magnifications.



(a) Light photomicrograph (oil immersion).



(b) SEM photomicrograph; secondary electron mode.

Figure 2. - Comparison of light optical and SEM photomicrographs of as-cast WAZ-20 specimen at X1700.

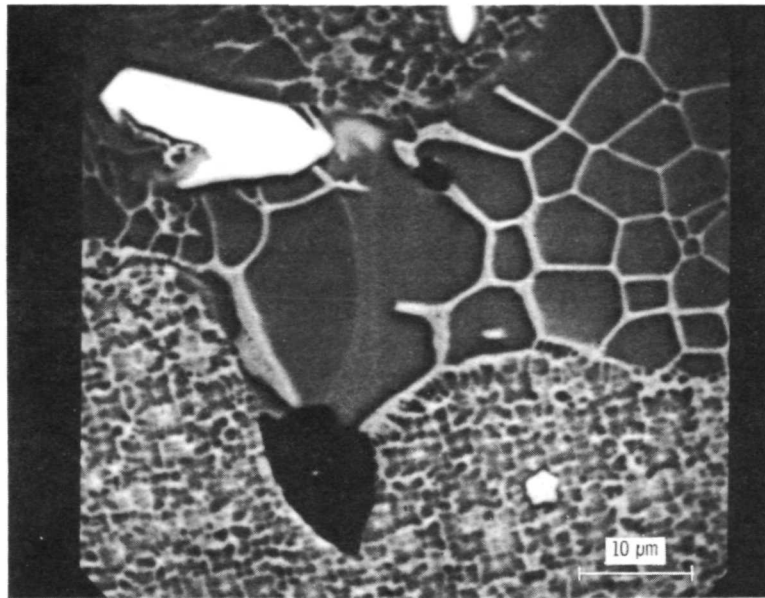
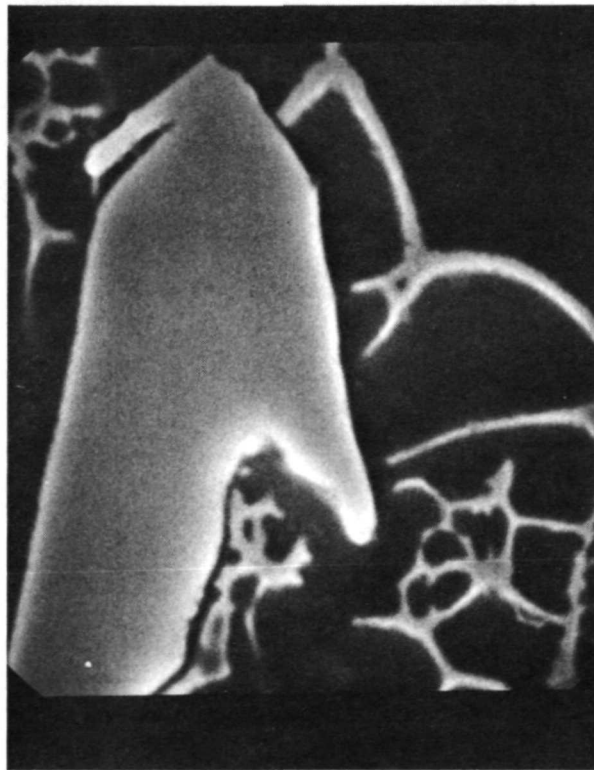
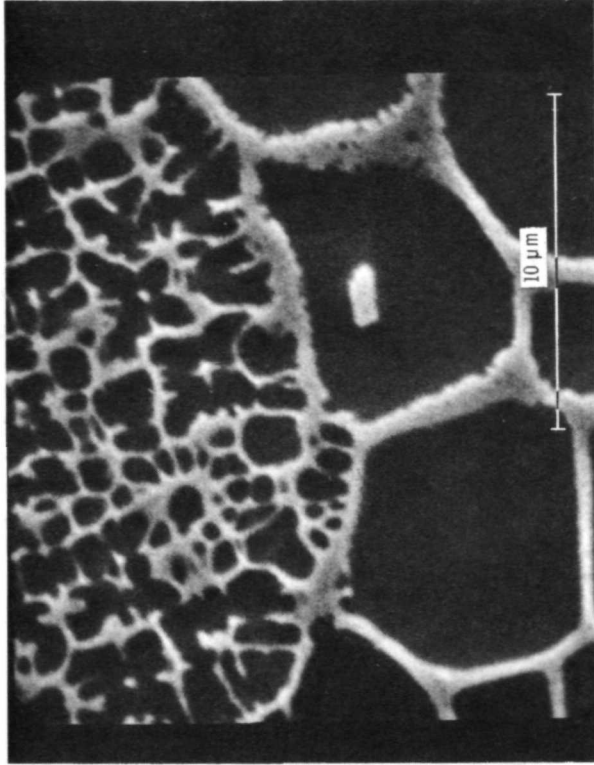


Figure 3. - SEM photomicrograph of as-cast WAZ-20 specimen at X1700 in backscatter electron mode (light regions indicate high concentrations of heavy elements).



(a) Carbide.



(b) Interface between coarse gamma-gamma prime eutectic and the gamma-fine gamma prime structure.

Figure 4. - SEM photomicrographs of as-cast WAZ-20 specimen at X5000 is secondary electron mode.

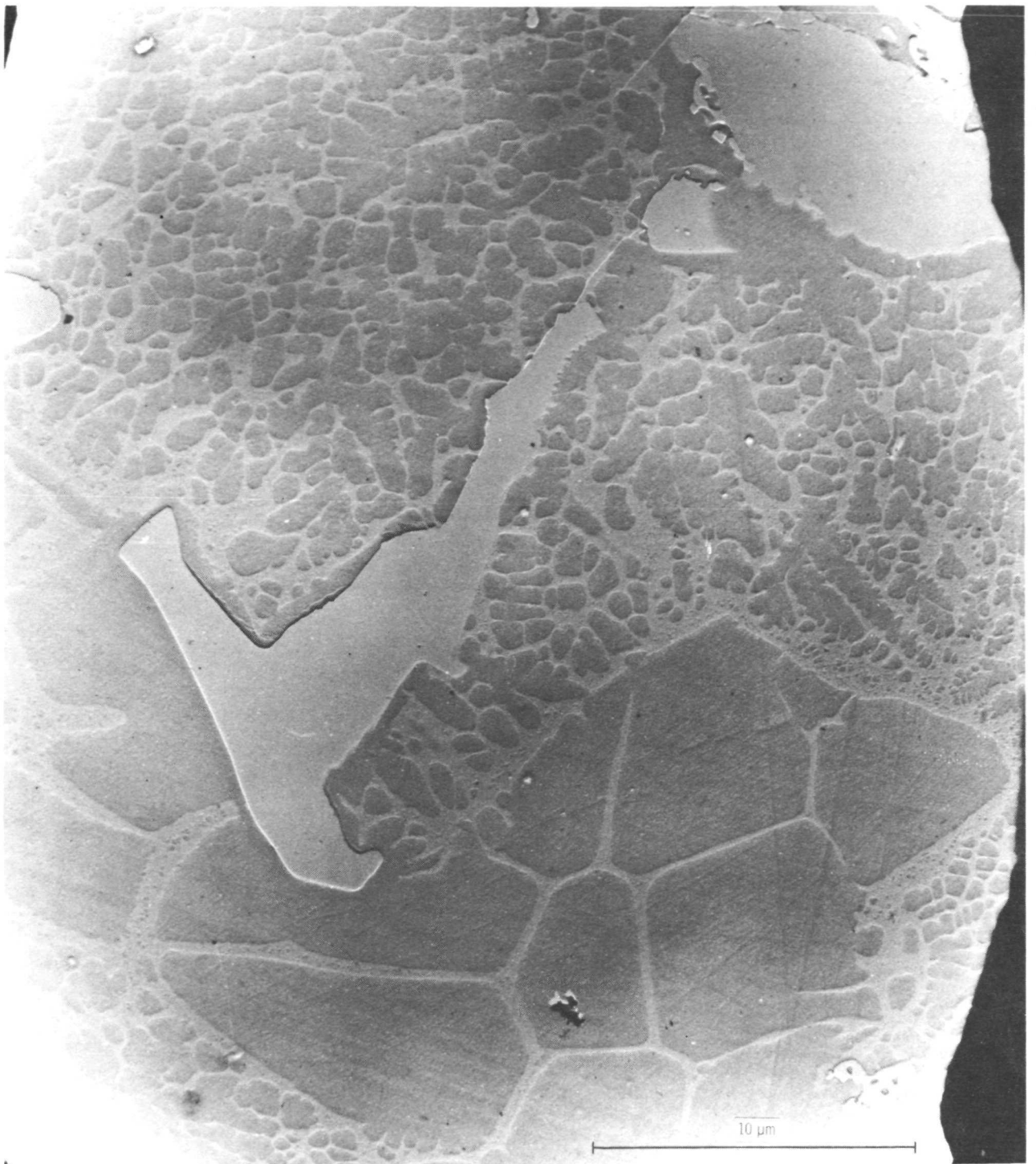


Figure 5. - Electron microscope photomicrograph of a replica from as-cast WAZ-20 specimen showing carbide, eutectic, and gamma-fine gamma prime structure at X6000.



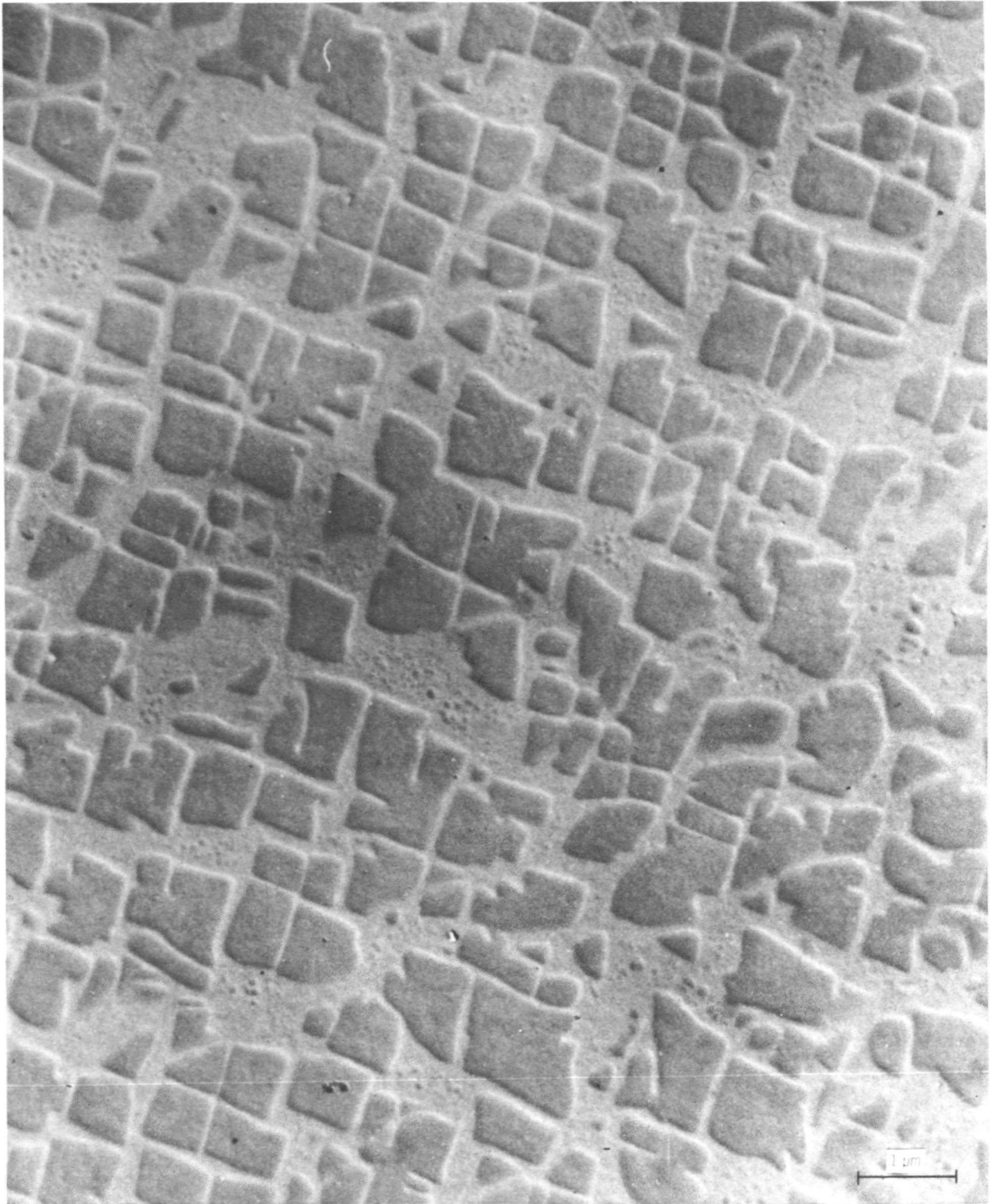
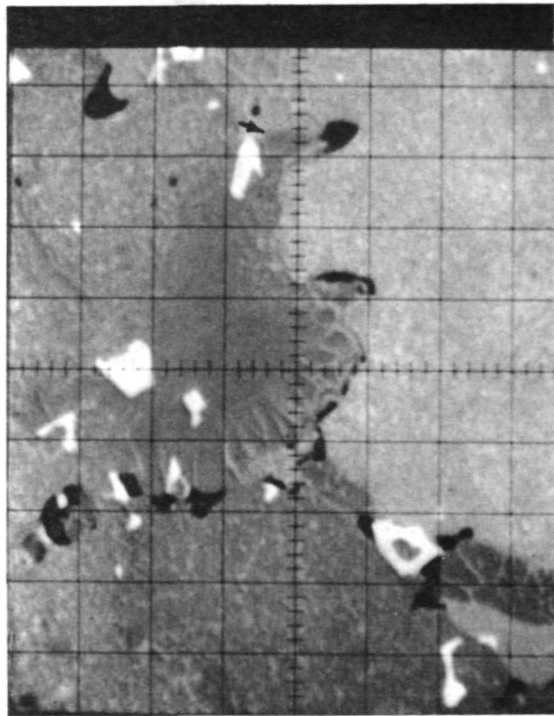
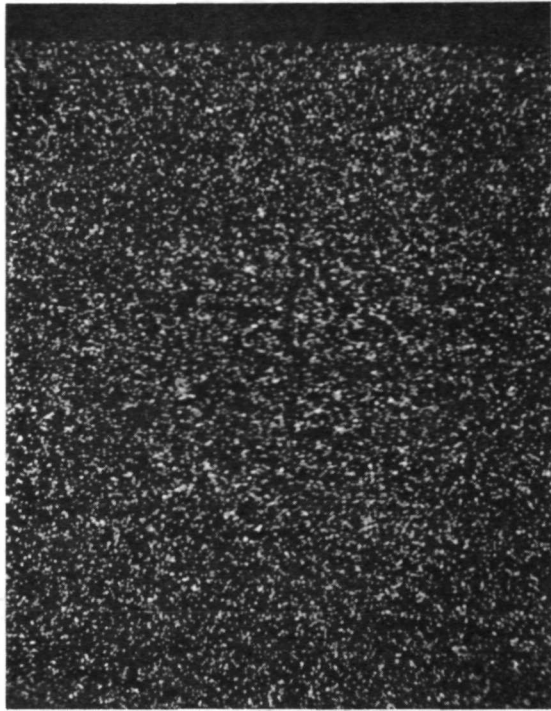


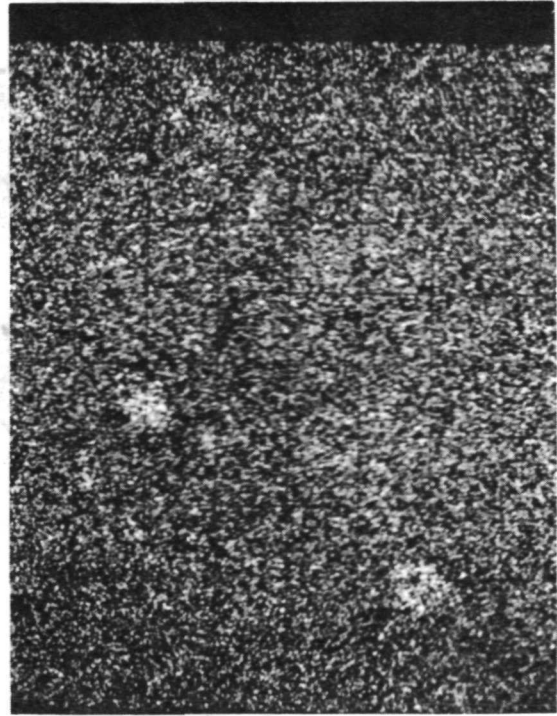
Figure 6. - Electron microscope photomicrograph of replica from the as-cast WAZ-20 specimen showing the gamma-fine gamma prime structure at X17000.



(a) Backscatter mode. Arrow shows apparent boundary between primary gamma prime and gamma prime associated with eutectic.



(b) Carbon.

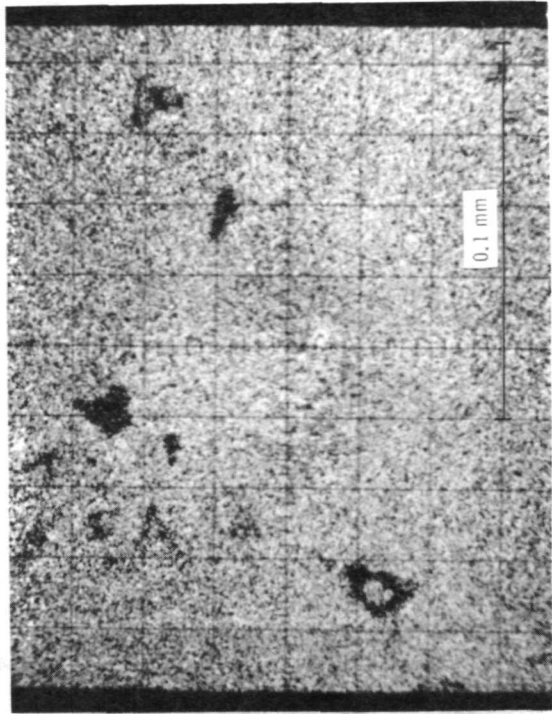
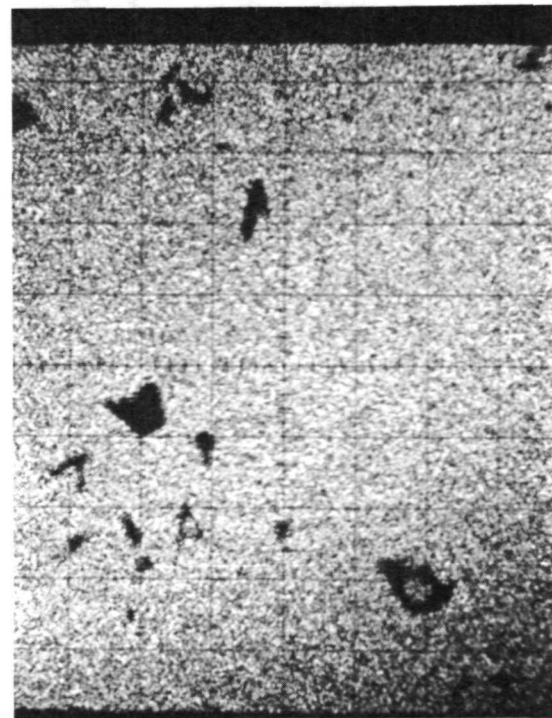


(c) Tungsten.



(d) Zirconium.

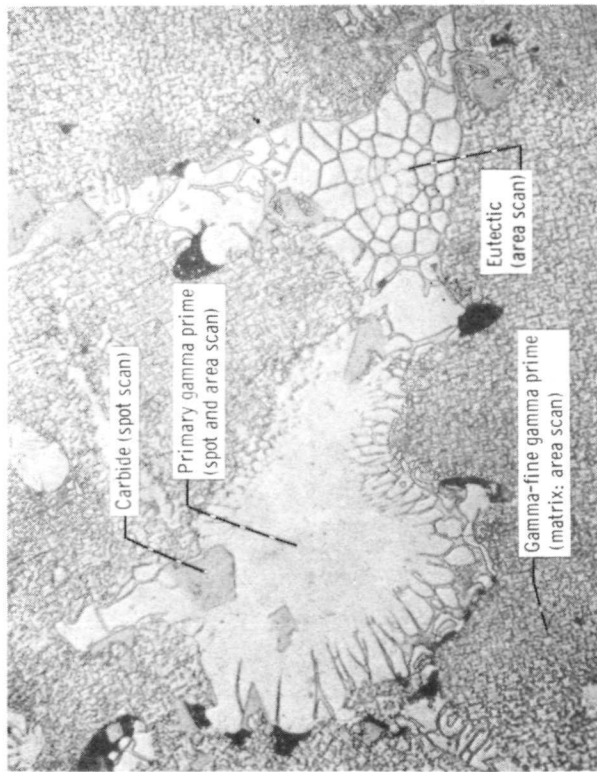
Figure 7. - EMXA photomicrographs of as-cast WAZ-20 specimen at X500 (approximately the same area as shown in the light photomicrograph of fig. 11c).



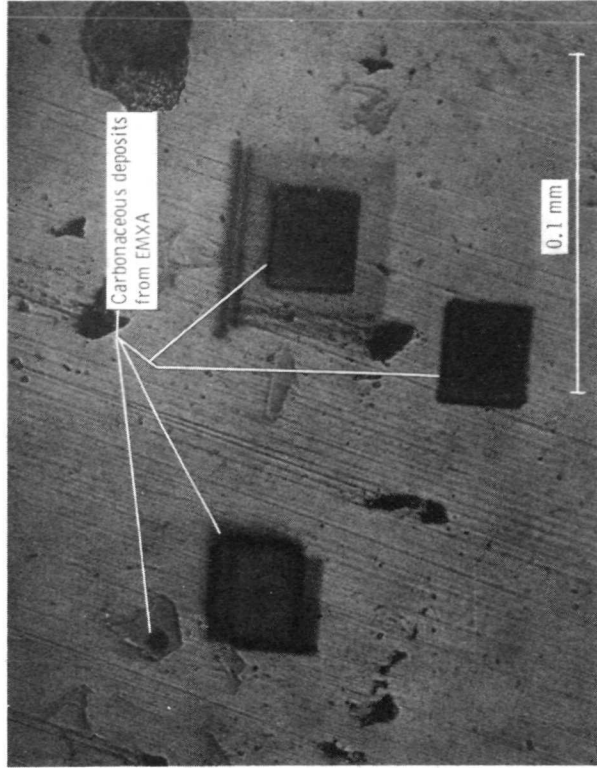
(f) Aluminum.

(e) Nickel.

Figure 7. - Concluded.

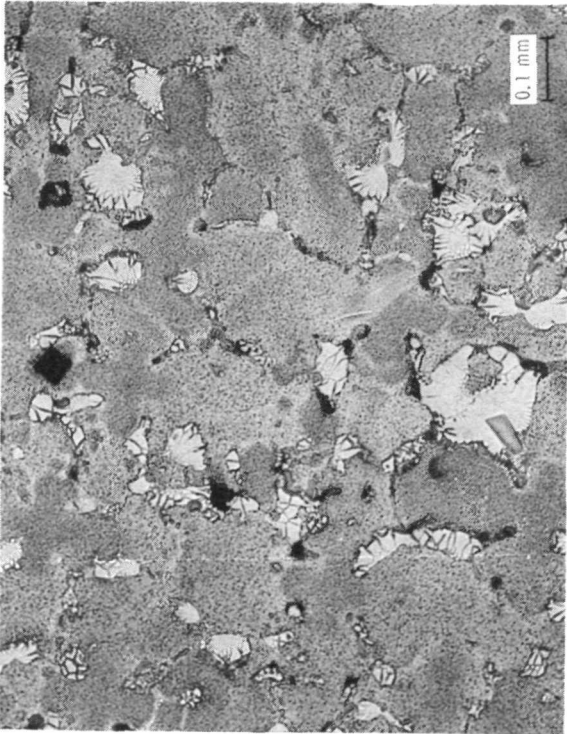


(a) Etched specimen showing primary gamma prime, carbides, eutectic, and gamma-fine gamma prime.

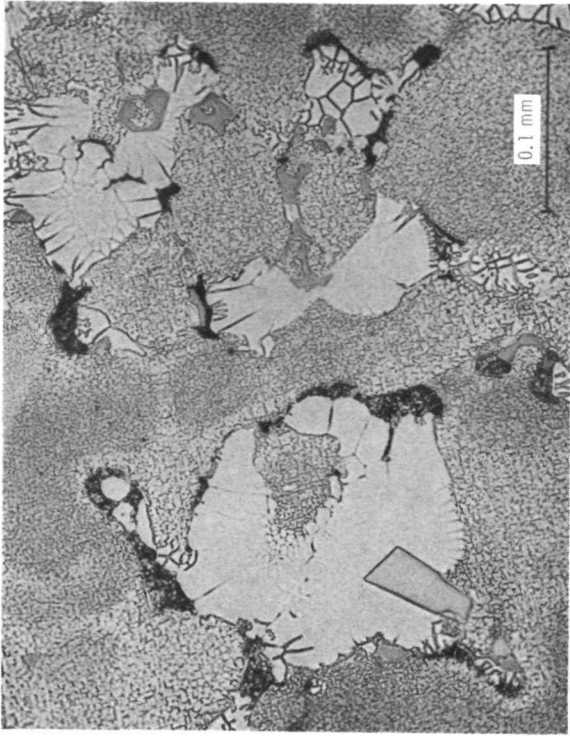


(b) Polished specimen of same area as (a) showing carbon deposits from EMXA quantitative analysis of constituents.

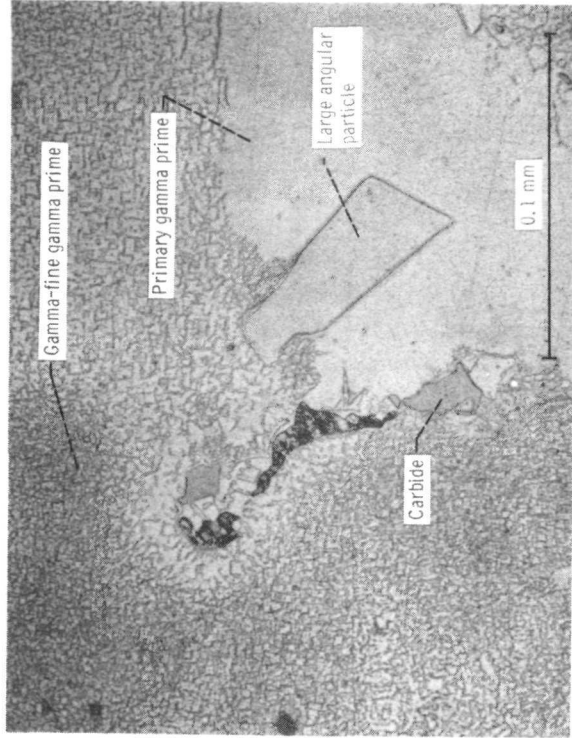
Figure 8. - Light photomicrographs of as-cast WAZ-20 specimen showing areas used for quantitative measurements by EMXA (X500).



(a) X100.



(b) X250.



(c) X500.

Figure 9. - Light photomicrographs of directionally solidified polycrystalline WAZ-20 aged for 1000 hours at 870° C.



POSTMASTER: If Undeliverable (Section 158  
Postal Manual) Do Not Return

*"The aeronautical and space activities of the United States shall be conducted so as to contribute . . . to the expansion of human knowledge of phenomena in the atmosphere and space. The Administration shall provide for the widest practicable and appropriate dissemination of information concerning its activities and the results thereof."*

—NATIONAL AERONAUTICS AND SPACE ACT OF 1958

## NASA SCIENTIFIC AND TECHNICAL PUBLICATIONS

**TECHNICAL REPORTS:** Scientific and technical information considered important, complete, and a lasting contribution to existing knowledge.

**TECHNICAL NOTES:** Information less broad in scope but nevertheless of importance as a contribution to existing knowledge.

**TECHNICAL MEMORANDUMS:** Information receiving limited distribution because of preliminary data, security classification, or other reasons. Also includes conference proceedings with either limited or unlimited distribution.

**CONTRACTOR REPORTS:** Scientific and technical information generated under a NASA contract or grant and considered an important contribution to existing knowledge.

**TECHNICAL TRANSLATIONS:** Information published in a foreign language considered to merit NASA distribution in English.

**SPECIAL PUBLICATIONS:** Information derived from or of value to NASA activities. Publications include final reports of major projects, monographs, data compilations, handbooks, sourcebooks, and special bibliographies.

**TECHNOLOGY UTILIZATION PUBLICATIONS:** Information on technology used by NASA that may be of particular interest in commercial and other non-aerospace applications. Publications include Tech Briefs, Technology Utilization Reports and Technology Surveys.

*Details on the availability of these publications may be obtained from:*

**SCIENTIFIC AND TECHNICAL INFORMATION OFFICE**

**NATIONAL AERONAUTICS AND SPACE ADMINISTRATION**  
Washington, D.C. 20546